

HEAT FLUX DETERMINATION FROM ULTRASONIC PULSE MEASUREMENTS

M.R. Myers and D.G. Walker*
Department of Mechanical Engineering
Vanderbilt University
Nashville, TN, 37235

D.E. Yuhas and M.J. Mutton
Industrial Measurement Systems, Inc.
2760 Beverly Drive, Suite 4
Aurora, IL 60502

ABSTRACT

Ultrasonic time of flight measurements have been used to estimate the interior temperature of propulsion systems remotely. All that is needed is acoustic access to the boundary in question and a suitable model for the heat transfer along the path of the pulse train. The interior temperature is then deduced from a change in the time of flight and the temperature dependent velocity factor, which is obtained for various materials as a calibration step. Because the acoustic pulse samples the entire temperature distribution, inverse data reduction routines have been shown to provide stable and accurate estimates of the unknown temperature boundary. However, this technique is even more interesting when applied to unknown heat flux boundaries. Normally, the estimation of heat fluxes is even more susceptible to uncertainty in the measurement compared to temperature estimates. However, ultrasonic sensors can be treated as extremely high-speed calorimeters where the heat flux is directly proportional to the measured signal. Through some simple one-dimensional analyses, this work will show that heat flux is a more natural and stable quantity to estimate from ultrasonic time of flight. We have also introduced an approach for data reduction that makes use of a composite velocity factor, which is easier to measure.

Introduction

Ultrasonic pulse measurements have been used in non-destructive evaluation (NDE) for decades with a great deal of success [1]. Furthermore, ultrasonic pyrometry has been used in many process control systems [2] because the sound speed is a strong function of temperature in most materials. This technique

has proven effective for gases [3], fluids [4] and extrusions [5] as long as direct access to the material where the temperature being measured is available. These applications are concerned with average temperature measurements and have not, in general, been used to extract transient heat fluxes.

Heat flux has been a difficult quantity to measure directly. Existing devices include thermopiles and calorimeters, but these merely measure temperature differences or transient changes in temperature in such a way that is presumably proportional to heat flux. Normally these devices have a thermal mass that limits measurements of high frequency components, require tedious calibration, and are intrusive devices that disturb the phenomena that is being measured. An alternative approach to obtaining heat flux is to measure temperature directly and use inversion techniques to recover heat flux [6]. This approach has the advantage of being able to acquire measurements with less disturbance and with high sample rates. However, heat flux estimates are sensitive to measurement noise, and subsequent data reduction is somewhat of an art.

The present work demonstrates how ultrasonic (US) pulses can be used to measure heat flux directly. Ultrasonic sensing has been used to measure average temperatures in homogeneous media, but have not been used to predict boundary heat flux directly. Unlike the other heat flux measurement approaches, the ultrasonic sensor is located away from the boundary of interest. Consequently, the phenomenon that is being measured is not disturbed. In addition, the sample rate is limited only by the speed of sound through the medium. Compared to inversion routines, the heat flux is obtained as an algebraic equation involving an easily measured quantity, namely, time of flight.

For demonstration purposes, we will limit the discussion to

*Address all correspondence to this author.

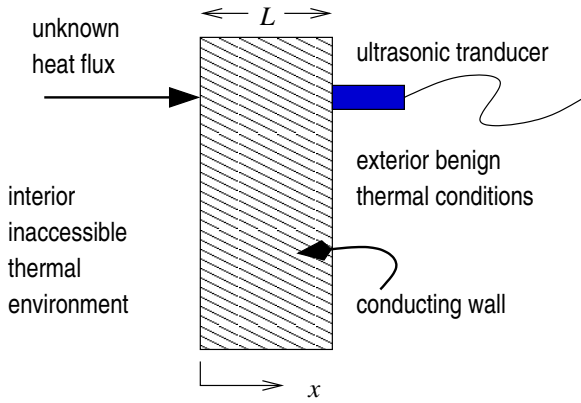


Figure 1. One-dimensional system with thermal boundary conditions through which an ultrasonic pulse propagates.

one-dimensional conduction domains with a single reflecting interface, which will be the surface where we want to know the heat flux. The opposite boundary will be assumed known and will be where the ultrasonic sensor is located. See Figure 1 for a schematic of the setup. Much of the development presented here can be extended to nonlinear, multi-dimensional problems, which are the focus of ongoing investigation, and are not provided in this preliminary look at the capability.

Development

In general, boundary temperatures can be recovered from ultrasonic (US) pulse data from a simple inversion routine operating on a suitable conduction model. The time of flight for a pulse through an isothermal, homogeneous medium is given as $G = 2L/v$, where L is the thickness of the medium and c is the speed of sound through the medium. The 2 accounts for the round trip time. If the medium contains temperature variations, then the time of flight is obtained by integrating the temperature-dependent sound speed over the thickness.

$$G = 2 \int_0^L \frac{1}{v(T(x))} dx = 2 \int_0^L \frac{1}{v_o[1 + P\theta(x)]} dx \quad (1)$$

In the foregoing expression, $P = (1/c)(\partial c/\partial T)$ is the velocity-temperature factor, which is a constant that describes how the velocity changes with temperature. c_o is the sound speed at some reference temperature T_o , and the change in temperature is relative to the reference as $\theta(x) = T(x) - T_o$.

This expression for time of flight is a common way of describing the variation in travel time for an ultrasonic pulse resulting from temperature fluctuations. In actuality, the length and velocity both change with temperature—the length because of the coefficient of thermal expansion (CTE, denoted as α here)

and the velocity because of the temperature dependent occupation of phonon frequencies. However, the two mechanisms are perfectly correlated, which means the effects can not be distinguished. Consequently, in the definition of time of flight, the two effects are usually lumped into a single parameter P . For the present development consider an alternative parameter ξ , which describes how the time of flight changes with temperature. Of course, this parameter also lumps the thermal expansion and velocity effects into a single parameter, but now the time of flight can be expressed as

$$G = \frac{2}{v_o} \int_0^L [1 + \xi\theta(x)] dx. \quad (2)$$

In the foregoing expression, the 2 accounts for the round-trip travel time as before, and $\theta(x) = T(x) - T_o$ is the temperature change relative to the reference.

The new parameter in equation 2 is defined as

$$\xi \equiv \frac{1}{G} \frac{dG}{dT} = \frac{1}{L} \frac{dL}{dT} - \frac{1}{v} \frac{dv}{dT} \quad (3)$$

The first term on the right hand side is the linear coefficient of thermal expansion for isotropic materials (α). The temperature dependence of the velocity can be approximated by writing the sound speed in a solid in terms of the Young's modulus and density ($v \equiv \sqrt{E/\rho}$), such that

$$\frac{1}{v} \frac{dv}{dT} = \frac{1}{2} \left[\frac{1}{E} \frac{dE}{dT} - \frac{1}{\rho} \frac{d\rho}{dT} \right]. \quad (4)$$

The second term is the volumetric coefficient of thermal expansion given as -3α . The temperature dependence on the Young's modulus is considered a constant [7], which we will define γ . Now our time of flight correction becomes

$$\xi = -\frac{1}{2}(\alpha + \gamma), \quad (5)$$

which is constant for a large number of materials over large temperature ranges.

Now the time of flight can be expressed as

$$G = \frac{2L}{v_o} + \frac{2\xi}{v_o} \int_0^L \theta(x) dx. \quad (6)$$

Although the resulting integral can still not be evaluated exactly, we recognize that the integral represents the total energy

added to the system relative to the reference energy. For a one-dimensional control volume of a solid medium with some heat transfer on both boundaries (see Figure 1), an energy balance on the slab shows that

$$q''(x=0) = \rho c_p \int_0^L \frac{\partial \theta(x)}{\partial t} dx + q''(x=L). \quad (7)$$

For short time periods we can approximate the time derivative as a difference such that

$$q''_0 = \frac{\rho c_p}{\Delta t} \int_0^L \Delta \theta(x) dx + q''_L, \quad (8)$$

where the subscripts 0 and L are used to identify the respective boundaries. The integral can be expressed in terms of ΔG obtained from equation 6, such that

$$q''_0 = \frac{\rho c_p}{\Delta t} \frac{c_0 \Delta G}{2\xi} + q''_L. \quad (9)$$

Equation 9 is significant because it relates an unknown and presumably inaccessible heat flux (q''_0) directly to a measurable quantity ΔG assuming we know what is happening on the accessible side (at $x=L$). Although many alternative approaches for measuring heat flux have been devised, the proposed approach offers several distinct advantages. 1) Unlike thermopiles and calorimeters, the transient response is limited only by the speed of sound—not the thermal mass of the sensor. 2) Unlike inversion of temperature measurements, the heat flux is computed from an algebraic equation, so measurement noise does not get amplified. 3) Measurements can be made remotely, which prevents the disturbance of the measured quantity and removes the sensor from the harsh thermal environment.

Analysis

To evaluate the efficacy of this method for measuring heat fluxes, we consider several special cases where the accessible boundary q''_L is known. In each case an analytic conduction solution is obtained for a prescribed boundary heat flux. From this temperature distribution a simulated time of flight is obtained by integrating the distribution as in equation 2. The thermal properties, dimensions and ultrasound coefficient ξ are assumed known. From the simulated time of flight, a heat flux is calculated. The calculated heat flux is then compared to the originally prescribed heat flux and errors are estimated. Figure 2 shows the process. In a measurement system, the heat flux is unknown, and the time of flight for two pulses separated by a time Δt would be used to obtain the calculated heat flux directly.

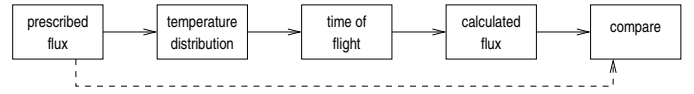


Figure 2. The process used to analyze the US heat flux sensor approach.

Table 1. Properties of a typical metal such as aluminum were used.

Property	Value
thermal conductivity (k)	250 W/m K
thermal diffusivity (κ)	$1.03 \times 10^{-6} \text{ m}^2/\text{s}$
sound speed (v)	4877 m/s
US coefficient (ξ)	$22.2 \times 10^{-6} \text{ m/m K}$

In reference to Figure 1, the side of the slab with the simulated prescribed flux ($x=0$) is identified as the interior side and the boundary at $x=L$ is identified as the exterior wall. This terminology is used because the application form which this measurement approach was developed is a container with thermal extreme environments on the inside. The US approach is being developed to measure the interior conditions from the outside of the container where conditions are much more benign.

For reference, the material properties used in the analysis are approximately those of aluminum and are given in Table 1. Non-dimensionalization was used where possible to generalize the results.

Constant heating

The first case involves a slab ($L=1$ cm) initially at a uniform temperature so that there is no heat transfer in the system. Now assume that a jump in heat flux ($q''_0 = 1 \text{ MW/m}^2$) is applied at $x=0$ and $t \geq 0$. After small times (small Fo), the temperature response and the heat transfer at $x=L$ will be negligible because the injected energy will not have had enough time to penetrate the slab. Therefore, $q''_L = 0$. The temperature solution is given as [8]

$$\frac{\theta(x,t)}{\theta_{SS}} = 1 - x^* - 2 \sum_{n=0}^{\infty} \frac{(-1)^n}{\beta_n^2} \sin[\beta_n(1-x^*)] \exp(\beta_n^2 \text{Fo}), \quad (10)$$

where $\beta_n = (2n+1)\pi/2$, $x^* = x/L$, and $\text{Fo} = \kappa t/L^2$. The temperature is normalized by the steady state temperature on the interior surface $\theta_{SS} = q''_L/k$. Figure 3 shows the ultrasonic calculated heat flux as a function of Fo for a prescribed heat flux of unity.

For $\text{Fo} < 0.05$, the slab behaves like a semi-infinite slab where the backside boundary condition does not affect the temperature distribution. In this limit, the flux leaving the slab at

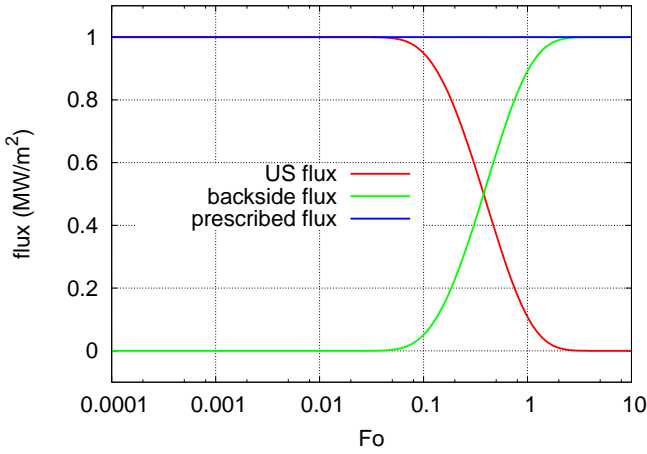


Figure 3. Simulated comparison between ultrasonic-derived (US) heat flux and a prescribed boundary heat flux of $1 \times 10^6 \text{ W/m}^2$. At $\text{Fo} \approx 0.05$, the backside flux (at $x = L$) becomes significant enough to affect the US flux.

$x = L$ is negligible and the US flux is a good estimate of the interior ($x = 0$) boundary heat flux.

Periodic heating

A steady-periodic solution was used to explore the ability of a US sensor to recover a varying heat flux. The prescribed flux at the interior surface is given as

$$\frac{q_0''(t)}{q_{\max}''} = \sin(2\pi t^* + \pi/4), \quad (11)$$

where time has been normalized by the period τ . The temperature distribution, which results from the applied flux and which is used to generate the time of flight, is

$$\frac{\theta(x,t)}{\theta_{\max}} = \exp(-x^*) \sin(2\pi t^* - x^*), \quad (12)$$

where $\theta(x,t) = T(x,t) - T_{\text{mean}}$, and $x^* = x/x_p$ is normalized by the penetration depth parameter $x_p = \sqrt{\kappa\tau/\pi}$. The maximum heat flux and maximum temperature are related by the period of the oscillations through x_p :

$$\frac{q_{\max}''}{\theta_{\max}} = \frac{\sqrt{2}k}{x_p}. \quad (13)$$

The integration of the temperature distribution and subsequent determination of the time of flight follows as in the constant heating case. For the steady-periodic test case, the depth of the slab,

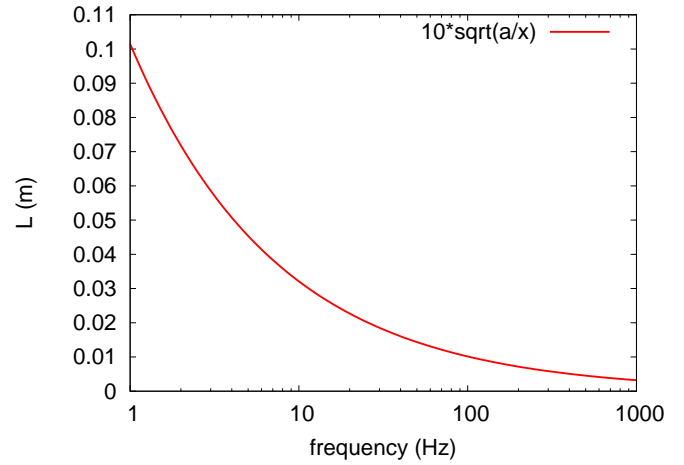


Figure 4. Threshold for slab thickness to justify a zero exterior heat flux assumption. The line produces an error $\sim 0.05\%$. Everything above the line gives smaller errors.

which is also the distance that the US pulse travels, was set so that the thermal oscillations did not extend to the exterior boundary. In this way, we can use the semi-infinite solution (equation 12) for the temperature distribution. For $L = 9x_p$, the effect of the boundary (error $< 0.05\%$) is reduced to the point that other numerical artifacts such as the numerical integration overwhelm the error in the estimate. Figure 4 shows the slab thickness that gives an error less than 0.05% for the assumption that $q_L'' = 0$. Everything above the line gives smaller errors. Note that the US measurement approach can still be used effectively for thinner slabs (below the line). In this case, though, the heat out of the exterior surface needs to be characterized to satisfy the energy balance (equation 2).

For the constant prescribed heat flux, the size of the Δt parameter does not affect the solution because the piecewise constant assumption matches the actual heat flux perfectly. However, if the prescribed flux varies, as in the steady-periodic case, the piecewise constant assumption could break down for large Δt . Figure 5 shows how the percent error increases as a function of the time between pulses normalized by the period ($\Delta t^* = \Delta t/\tau$). The percent error is calculated as the maximum difference between the prescribed and US heat flux normalized by the maximum flux ($q_{\max}'' = 1 \text{ MW/m}^2$):

$$\% \text{error} = 100 \times \max \left[\frac{|q_{\text{prescribed}}'' - q_{\text{US}}''|}{q_{\max}''} \right]. \quad (14)$$

Figure 5 allows us to determine the highest frequency of the heating load that is resolvable for a given time between pulses and to estimate the error associated with the measurement.

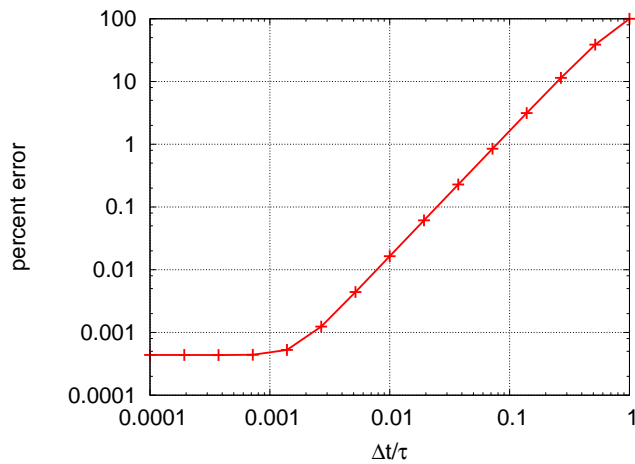


Figure 5. Error induced in the US sensor method due to piecewise constant assumption over various $\Delta t^* = \Delta t/\tau$.

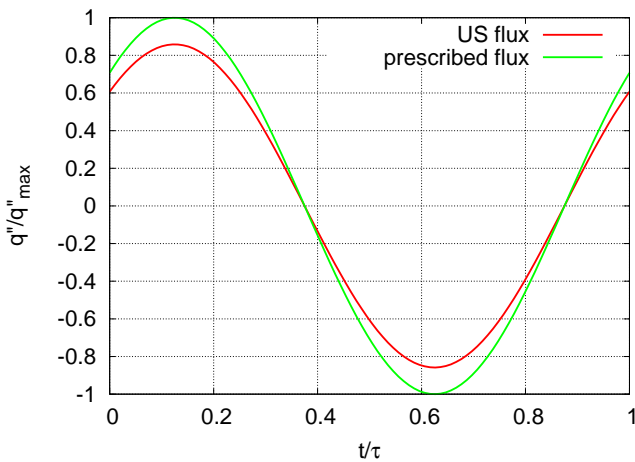


Figure 6. When the time step becomes too large ($\Delta t = 0.3\tau$), the US sensor underestimates the peak of the oscillatory heat flux.

For a relatively poor choice of $\Delta t^* = 0.3$, Figure 5 shows that the percent error should be about 20%. Figure 6 shows the simulated flux estimate from the US sensor compared to the prescribed flux. The US sensor underestimates the magnitude of the prescribed flux uniformly.

Conclusions

We have shown that ultrasonic time of flight data can be used to estimate remote boundary fluxes without an inversion step. However, the foregoing analysis assumes a one-dimensional system. The technique could likely be extended to multiple dimen-

sions as long as all conditions other than the unknown boundary being measured are known. In addition, the approach assumes that the new parameter ξ is a material property and is constant. This assumption should be tested for various materials. Nevertheless, we are confident that the combined parameter L/v is linear in temperature, which would suggest that ξ is constant.

The time of flight approach is an effective remote sensing technology because, unlike normal inverse heat conduction problems, the US pulse samples the entire temperature distribution instead of measuring a single point temperature. As such, a change in the time of flight from one pulse to the next is really a measure of the stored energy in the system. If all other heat transfers are known (in particular, the generated and accessible boundary flux), then the unknown heat flux can be calculated from an energy balance.

Experimental tests need to be performed on these canonical systems to characterize the noise associated with the time of flight measurement and autocorrelation of the signal. Modern 12-bit high-speed US measurement systems are capable of extremely high sample rates with little noise. In fact preliminary tests have shown that noise levels are easily below uncertainties in many of the parameters used in this analysis. Nevertheless, these noise levels still need to be analyzed.

REFERENCES

- [1] Yee, B. G. W., and Couchman, J. C., 1976. "Application of ultrasound to NDE of materials". *IEEE Transactions on Sonics and Ultrasonics*, **SU-23**(5), Sept., pp. 299–305.
- [2] Hoyle, B. S., and Luke, S. P., 1994. "Ultrasound in the process industries". *Engineering Science and Education Journal*, **3**(3), pp. 119–122.
- [3] Green, S. F., 1985. "An acoustic technique for rapid temperature distribution measurements". *Journal of the Acoustical Society of America*, **77**(2), Feb., pp. 759–763.
- [4] Fife, S., Andereck, C. D., and Rahal, S., 2003. "Ultrasound thermometry in transparent and opaque fluids". *Experiments in Fluids*, **35**, pp. 152–158.
- [5] Chen, G., 1999. "Phonon wave heat conduction in thin films and superlattices". *Journal of Heat Transfer*, **121**, Nov., pp. 945–953.
- [6] Beck, J. V., Blackwell, B., and St. Claire Jr., C. R., 1985. *Inverse Heat Conduction: Ill-Posed Problems*. Wiley-Interscience.
- [7] Liu, J. M., 1984. "Temperature dependence of elastic stiffness in aluminum alloys measured with non-contact electromagnetic acoustic transducers (EMATs)". In *IEEE Ultrasonics Symposium*, pp. 972–974.
- [8] Carslaw, H. S., and Jaeger, J. C., 1959. *Conduction of Heat in Solids*, 2nd ed. Oxford Science Publications.